Chapter 4
Adaptive Control Strategies for Productive Toner Printers

Paul van den Bosch, Carmen Cochior, Mohamed Ezzeldin, Perry Groot, Peter Lucas, Jacques Verriet, René Waarsing, and Siep Weiland

Abstract This chapter discusses design considerations for industrial systems and processes when embedded systems allow to intelligently influence the system in real-time. It is shown that in such embedded systems the capability to adapt themselves to changing environments and/or to different operating conditions has to be exploited. If properly done, almost all performance indicators like accuracy, speed, robustness, insensitivity for disturbances, will improve. The challenge is to first study the process for which the behaviour has to be improved. Based on the characteristics of the process and its disturbances, one wishes to select among the hundreds of tools to achieve its goals. For the professional printer, this design process and its many compromises and choices will be illustrated. Consequently, the professional printer will be analysed for its specific characteristics whose behaviour can be influenced during printing. Based on these characteristics, appropriate control approaches are discussed in more detail to show how control can cope with uncertainty or changing parameters. With extensive and illustrative examples the

P. van den Bosch (✉) • C. Cochior • M. Ezzeldin • S. Weiland
Control Systems group, Faculty of Electrical Engineering, Eindhoven University of Technology, P.O. Box 513, 5600 MB Eindhoven, The Netherlands
e-mail: p.p.j.v.d.bosch@tue.nl; c.cochior@tue.nl; m.ezz@tue.nl; s.weiland@tue.nl

P. Groot • P. Lucas
Department of Model-Based System Development, Institute for Computing and Information Sciences, Radboud University Nijmegen, P.O. Box 9010, 6500 GL Nijmegen, The Netherlands
e-mail: perry@cs.ru.nl; peterl@cs.ru.nl

J. Verriet
Embedded Systems Institute, P.O. Box 513, 5600 MB Eindhoven, The Netherlands
e-mail: jacques.verriet@esi.nl

R. Waarsing
Océ-Technologies B.V., P.O. Box 101, 5900 MA Venlo, The Netherlands
e-mail: rene.waarsing@oce.com

T. Basten et al. (eds.), *Model-Based Design of Adaptive Embedded Systems*, Embedded Systems 22, DOI 10.1007/978-1-4614-4821-1_4,

various methods are compared and it is shown why some control approaches are preferred solutions in the large number of problems that are faced by professional printers.

4.1 Introduction

Dealing with uncertainty in physical processes can be solved in several ways. One way is to assume that the process behaves reasonably well and behaves more or less predictable. Then, a deterministic, nominal model with all uncertainty mapped in unknown disturbances can be derived either by using first-principle physical knowledge or by estimating an appropriate model based on measurements from appropriately selected experiments performed on that system. Another approach is needed when it is assumed that a deterministic model is unfeasible. In that case, all we have are measurements of a complex, unpredictable process. Based on these measurements, an attempt can be made to describe the process behaviour with a stochastic and/or statistical model, such as a Gaussian stochastic model or as a statistical Markov chain.

In both cases, control is an excellent approach as it delivers high performance to systems even when parameters of the system change and/or disturbances start to deteriorate system behaviour.

Basically, accurate models and/or accurate measurements are needed to guarantee that the output of a process satisfies the required values. Let us first introduce some variables to show the consequences of modelling and measurement errors. We define an input u, output y, disturbance w, and a reference value for the required output r. Let us assume that the process can be accurately represented as H_0, that we can find an approximate model H of the process and that we have designed a controller C. The measured output y of the real process will be $y = H_0 \cdot u + w$. That is, the measurement is a noise-corrupted output of the process that is controlled by the input u. If we rely on the knowledge of the approximate model H, an appropriate input u for the process that achieves the reference r as its output could be $u_{\mathrm{FF}} = H^{-1} \cdot r$, where the subscript FF indicates feedforward. Now the actual output of the process will become:

$$y = H_0 \cdot u_{\mathrm{FF}} + w = H_0 \cdot (H^{-1} \cdot r) + w. \tag{4.1}$$

It can be observed that when we accurately know the process, so $H = H_0$, and there are no disturbances, so $w = 0$, this feedforward value u_{FF} of u, yields that the output equals the reference value, so $y = r$. To establish this, no measurements are needed, ONLY an accurate model H of H_0 and NO disturbance. However, this chapter deals with systems and processes that are not accurately known or are time varying during the operation of the system, so $H_0 \neq H$, and when disturbances act on the process, so $w \neq 0$. Consequently, another approach has to be taken as illustrated in Fig. 4.1.

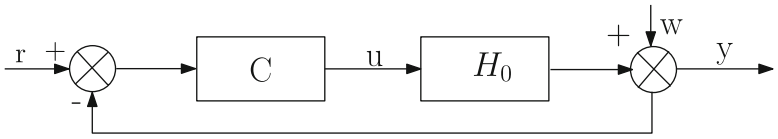

Fig. 4.1 Closed-loop control system

We can no longer rely only on accurate models. Measurements have to be used too. When using measurements of the output we can calculate the error e between the required value r and the actual value y, with $e = r - y$. If we use a feedback controller C to calculate an appropriate value of the input u for the process based on the error e, the control input u will be $u = C \cdot e$, and we will have the following relations:

$$y = H_0 \cdot u + w = H_0 \cdot C \cdot e + w, \tag{4.2}$$

$$y \cdot (1 + H_0 \cdot C) = H_0 \cdot C \cdot r + w, \tag{4.3}$$

$$y = \frac{H_0 \cdot C}{1 + H_0 \cdot C} \cdot r + \frac{1}{1 + H_0 \cdot C} \cdot w. \tag{4.4}$$

When properly designed, the value of the controller C will be (very) large within the area we want to control the process, yielding $H_0 \cdot C \gg 1$. Consequently $y = r$. This last result shows the power of control when both the model of the process is not correct ($H_0 \neq H$) and disturbances act on the process ($w \neq 0$). When accurately measured and an appropriate controller is designed, we can guarantee that the output y of the process will follow the required value r. In this setting, control looks like magic. It is not. Two major requirements are posed:

- A sufficiently accurate, but not exact, model is needed to design the controller C. Errors of 10–50% are allowed, but the basic dynamics have to be captured correctly.
- The measurements have to be accurate. If measurement noise is present, the control performance deteriorates accordingly.

Within the control area several approaches exist to cope with different classes of uncertainty and disturbances with advanced feedback controllers. These approaches are called Optimal, Robust, and Adaptive control. We discuss these approaches first.

- In an *optimal control* approach, the best controller is designed based on accurate knowledge of the process and its environment. If the uncertainties are explicitly known, the best controller is designed. The performance will be high, but if the assumptions about process or environment are not correct, the performance will deteriorate quite fast. It is not the best way to deal with uncertainty or changing operating conditions when uncertainty is dominant.

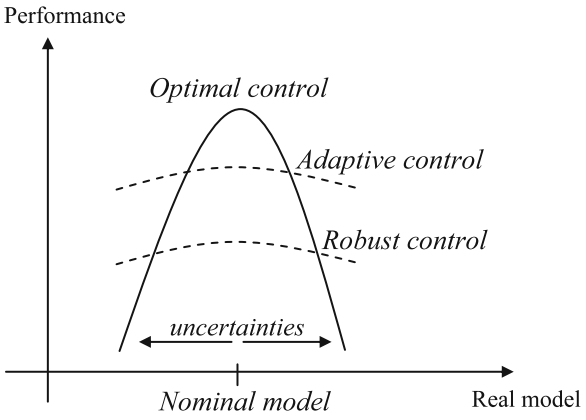

Fig. 4.2 Qualitative comparison of Optimal, Robust, and Adaptive control

- In a *robust design* the goal is to predict all possible deviations that can occur. Then, a controller is synthesised that can still deliver an acceptable performance even in the worst situation. So, the design is inherently conservative. There is always a trade-off between robust stability and robust performance. Therefore the price to be paid for increased robustness with respect to stability is a reduction in performance.
- An attractive alternative of robust control is *adaptive control*. Then, the controller explicitly or implicitly estimates the changing parameters or changing disturbances and adapts itself to the newly estimated situation. Within the new situation it can still achieve high performance. As it adapts itself to changing parameters and disturbances, it can be shown to be robust. In that sense adaptive control combines the advantages of optimal control (high performance) with those of robust control (insensitive for a changing environment). However, adaptive control requires an intensive on-line computation and it is sensitive to measurement noise.

In Fig. 4.2 the relative behaviour of Optimal control, Robust control, and Adaptive control is elucidated. It represents the expected performance of those controllers as functions of the changes in parameters and disturbances.

In the sequel, we will discuss how to select appropriate design approaches for a professional printer.

4.2 Characteristics of an Industrial Electro-Photography Printer

In this section, we try to describe and analyse the characteristics of industrial toner-based printers. Knowing these characteristics it is possible to select appropriate control approaches. First a short description of the physics behind electro-photography printers.

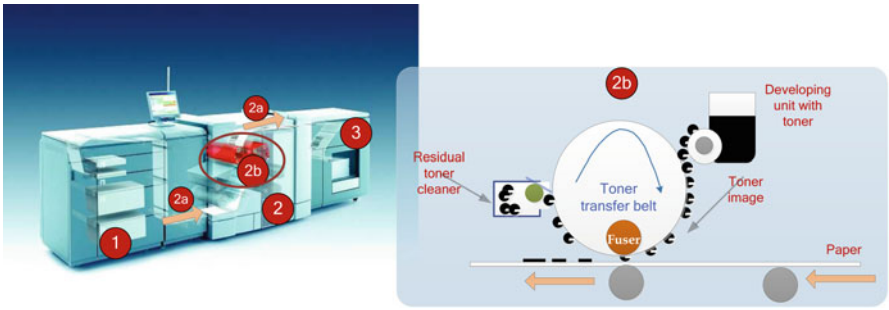

Fig. 4.3 Electro-photography printer: *1*. Paper input; *2*. Print engine: *a*. Paper path, *b*. Printing process; *3*. Finisher

4.2.1 Heat Flow Model

The printing process consists of six main steps: (1) charging of a photo-conductor, (2) exposing the photo-conductor drum or belt to the image, (3) development of the latent image, (4) transferring the image from the photo-conductor to a sheet of paper or any other printing media, (5) fusing the developed image to the printing media, and finally (6) cleaning any residual toner from the photo-conductor drum or belt in preparation for the next print [6, 13, 30]. These main steps are illustrated in Fig. 4.3. From the input tray the paper is transported first via a preheater along the toner belt with toner to the fusing point. Subsequently, it is transported to the output tray.

An important step, and the topic of this chapter, is the thermal process to fuse the toner on the paper. The temperature of fusing is very important. When this temperature is too low, the toner will not penetrate the paper and can easily be removed from the paper. If the temperature is too high, the toner will melt to any surface and, consequently, not always at the intended positions on the paper.

The thermal behaviour of a toner-based printer can be modelled with two elements, the thermal capacity C [J/K] and the thermal resistance R [K/W]. The thermal capacity is a buffer of the thermal energy $E = C \cdot T$ [J] with the temperature T [K] as variable which determines the energy stored in that buffer [20]. Basically, the following equations are valid with P [W] the thermal power flow. The time derivative of the temperature is proportional to the net incoming power flow P and the temperature difference is also proportional to the power flow P through the thermal resistor R:

$$\begin{aligned} \dot{T} &= \frac{1}{C} P, \\ T &= R P. \end{aligned} \tag{4.5}$$

Here, $\dot{T}$ stands for $\frac{dT}{dt}$, the time derivative of the temperature.

In the printing system, thermal power (heat) is transported in three different ways, namely, conduction, convection, and radiation. The heat is transported by conduction through the mechanical components. Heat flow is convected via air flow, and radiated by hot surfaces. In addition, heat is transported via the movement of objects in the printer, such as the printing media or the transport system.

Heat conduction and convection are modelled as linear thermal resistances, where the resistance may depend on system parameters such as rotational speed [16]. Heat radiation is modelled as a non-linear resistance. Heat, which is inserted into the printer, is represented as electric power. The printing system, which we study in this chapter, has two heaters that generate heat from electrical energy. The preheater, P_{pre}, is responsible for heating up the paper to a desired temperature before fusing. The toner transfer belt (TTF) rollers are usually heated using a tungsten quartz lamp P_{TTF}.

The following assumptions are made to derive the thermal model (4.6) below.

- The printer is modelled as a lumped component, where the description of the behaviour of the spatially distributed thermal system is simplified by an electrical circuit consisting of discrete entities that approximate the behaviour of the distributed system under certain assumptions. This approximation is useful to simplify complex differential heat equations. In this model, only the most interesting temperatures are explicitly included.
- The sheets are not modelled individually but as a continuous paper mass flow, which interacts with the preheater and the TTF belt.
- The interaction between areas of different temperatures are modelled using thermal resistance R between the temperatures of the lumped thermal capacities C.
- The printing media (the paper) extracts heat from the preheater and exchanges heat with the TTF.

A schematic view of the process can be seen in Fig. 4.4, where the printing media size is given by a length l [m] and a width b [m], while d [m] denotes the distance between two printing media.

As mentioned, controlling the fuse temperature is the key to achieve high print quality. The fuse temperature T_{fuse} is determined by the temperature of the paper sheets and the temperature of the TTF belt at the fuse pinch. The fuse temperature cannot be measured. Therefore, the preheating temperature T_{pre} and the TTF temperature T_{TTF} are used as a good estimation of the fuse temperature. The dynamics of the preheating and TTF systems are given by the following lumped model [16, 17].

$$\dot{T}_{\text{pre}} = \frac{1}{C_{\text{pre}}}\left(P_{\text{pre}} - m_{\text{pap}} v c_{\text{pap}}(T_{\text{pap}} - T_{\text{init}}) - \frac{T_{\text{pre}} - T_{\text{env}}}{R_{\text{env}}}\right),$$

$$\dot{T}_{\text{TTF}} = \frac{1}{C_{\text{TTF}}}(\eta_{\text{TTF}} P_{\text{TTF}} - \frac{T_{\text{TTF}} - T_{\text{env}}}{R_{\text{env}}} - \frac{T_{\text{TTF}} - T_{\text{pap}}}{R_{\text{pap}}} - \frac{T_{\text{TTF}} - T_{\text{slow}}}{R_{\text{slow}}} - \frac{T_{\text{TTF}} - T_{\text{roller}}}{R_{\text{roller}}}),$$

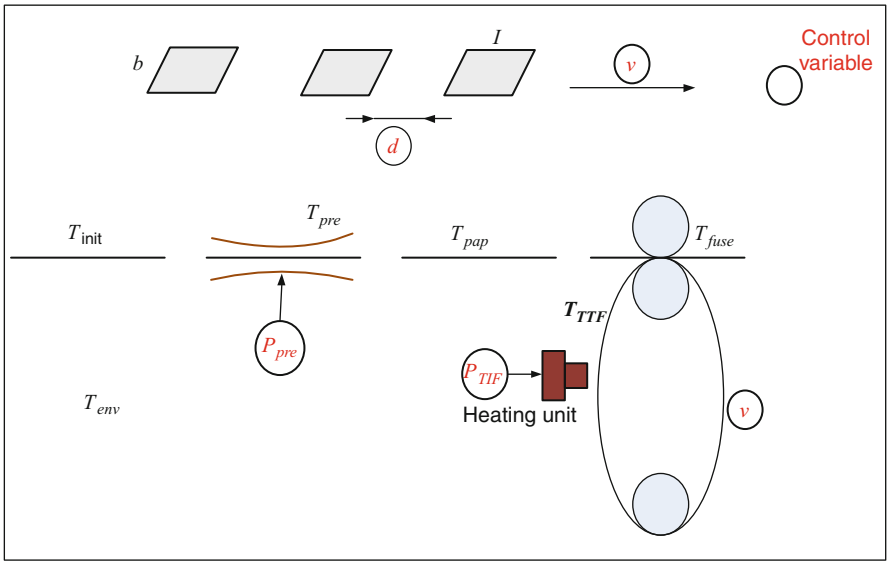

Fig. 4.4 Schematic view of the printer hardware

$$\dot{T}_{\text{roller}} = \frac{1}{C_{\text{roller}}}\left(\frac{T_{\text{TTF}} - T_{\text{roller}}}{R_{\text{roller}}}\right),$$
$$\dot{T}_{\text{slow}} = \frac{1}{C_{\text{slow}}}\left(\frac{T_{\text{TTF}} - T_{\text{slow}}}{R_{\text{slow}}}\right), \tag{4.6}$$

with

$$T_{\text{pap}} = T_{\text{init}} + (T_{\text{pre}} - T_{\text{init}})(1 - e^{\frac{-\lambda L_{\text{pre}}}{m_{\text{pap}} v}}),$$

where T_{init} is the paper temperature when entering the printer, C [J/K] represents the thermal capacity of the corresponding object, R [K/W] is the thermal resistance of the corresponding object, P_{pre} [W] and P_{TTF} [W] denote the input power to the preheater and the TTF heater, respectively, η_{TTF} [−] denotes the TTF heater thermal efficiency, m_{pap} [kg/m] is the paper mass per unit length, v [m/s] is the belt speed, T_{pap} [K] is the average temperature of the paper, and L_{pre} [m] represents the length of the preheater. T_{roller} [K] and T_{slow} [K] represent the temperatures of the various rollers that are in contact with the TTF. T_{env} [K] denotes the temperature of the environment to which thermal power is leaked.

An estimation formula is used to estimate the fuse temperature. The fusing system can be described by

$$T_{\text{fuse}} = h(T_{\text{pre}}, T_{\text{TTF}}, P_{\text{pre}}, P_{\text{TTF}}, v, d). \tag{4.7}$$

Due to reasons of industrial confidentiality, the details of the fusing model are omitted here. The model (4.6) is connected to a higher-level controller, which determines the amount of available power, the printer speed, and the distance between sheets. Several parameters of the model (4.6) are time varying, since these parameters depend on the different printing jobs and the rotation speed, while other parameters are unknown.

4.2.2 Characteristics Determining the Control Problem

In the previous section, a deterministic lumped model of the electro-photography printer has been formulated. It is only valid when all the stated assumptions are true and all parameters are known. A priori, we know that this model is a valid but rough approximation, as the assumptions may not be valid in practice. But, as described in the previous section, when applying control it is possible to cope with these model deviations and unmodelled disturbances. First we will describe the disturbances w acting on the printer and that influence the fuse temperature.

The following disturbance components can be distinguished in the variable w:

- The print jobs defined by the user require different paper sheets, each represented by its thermal and mechanical characteristics such as mass [gr/m^2], size, humidity, surface, and initial temperature. Between jobs, but also within a print job, different sheets of paper can be selected. That indicates that the temperatures in the printer are highly influenced by the arrival of sheets into the printer. Heavy and large sheets require much more thermal power (and so electric power for the heaters) to reach the required temperature of the fuse. From a control point of view these print jobs, stored in the *print queue*, will disturb the thermal process considerably. The changes are fast (changing stepwise) and large. Owing to the large thermal capacities in the printer and the limited amount of electrical power, it is difficult to cope with these large changes. However, there is one big advantage. The print jobs in the print queue are known in advance. It is possible to anticipate the disturbing effect of the different sheets in the print queue. When more heavy sheets are expected, the temperatures can already be raised to cope with their higher demands for thermal power in the future. The major influence of different sheets of paper are changing parameters of the printer (thermal capacities and resistances) and different power losses to the environment.
- At *cold start*, the printer has to be heated up initially before the first sheet can be printed. During a cold start the printer will run, but without sheets, to get equally heated components and belts inside the printer. Without paper, the parameters of the printer (thermal capacities and resistances) have considerably different values.
- The *environment temperature* determines the thermal power loss of the printer. It is not measured, but any controller has to cope with its influence. Although unknown, the environment temperature will not change quickly. A controller has to compensate its influence.

- An even slower process is *wear*. At a longer time scale it will change the process parameters owing to aging, pollution and degrading performance of subsystems. A controller has to take care of slowly changing parameters and counteract them.

Next we discuss the control inputs u. The inputs $u = (P_{\text{pre}}, P_{\text{TTF}}, v, d)$ can be manipulated freely to influence the system. These input are generated by a controller to compensate all disturbances mentioned, such that print quality is not sacrificed and print throughput is still at a maximum. The measured outputs y include the preheating temperature T_{pre} and the TTF temperature T_{TTF}. That is $y = (T_{\text{pre}}, T_{\text{TTF}})$. With reference to the heat model (4.6), the system states x are defined in a 4-dimensional vector

$$x := \begin{bmatrix} T_{\text{pre}} \\ T_{\text{TTF}} \\ T_{\text{roller}} \\ T_{\text{slow}} \end{bmatrix}.$$

- Both the preheater and the TTF belt can be heated with separate electrical powers (P_{pre} and P_{TTF}). The maximum current of a power connection is specified, while the voltage, and so the power, can change. However, both have a maximum and together they have to satisfy the maximum amount of electrical power for heating. The maximum can change owing to other, higher priority jobs inside the printer.
- When heavy paper sheets are being printed, it requires more thermal and so more electrical power to heat these sheets to the required temperature. When the constraint on electrical power is active, the same temperatures can still be achieved by either decreasing the print speed v or by increasing the distance d between the sheets.

The following constraints have to be satisfied.

- Input constraints: power, velocity, and distance are considered variable according to

$$P_{\text{pre}}(t) + P_{\text{TTF}}(t) \leq P_{\max}(t), \tag{4.8}$$

$$|\Delta v(t)| \leq \overline{v}, \tag{4.9}$$

$$v_{\min} \leq v \leq v_{\max}, \tag{4.10}$$

$$d_{\min} \leq d \leq d_{\max}. \tag{4.11}$$

  where $\Delta v(t)$ is the change rate of velocity.
- Print process constraints: tight bounds for the fuse temperature to guarantee a minimum print quality.

The goal will be to maximise throughput Λ [ppm] while satisfying print quality (fuse temperature constraints) and all technical constraints, such as the maximum available electrical power. Throughput Λ depends on the velocity v of the printer

and on the sheet length l and the distance d between two sheets:

$$\Lambda = \frac{60v}{l+d}. \tag{4.12}$$

To achieve that goal, one consistent and transparent problem formulation with all aspects operating a printer has to be considered. Solving this large optimisation problem will result in the optimal compromise between all conflicting requirements.

Looking at the characteristics of the disturbances it can be noted that a printer changes its behaviour considerably during printing. Especially the fast changes in requested paper sheets, introduce large changes in the parameters of the printer. Consequently, one optimal controller for all operating conditions cannot be expected to deliver the required print quality. The large changes demand a robust or an adaptive controller. The slowly varying environment temperature and the consequences of wear can be taken into account by many controllers.

A high throughput is required. Consequently, at some point in time the operation will hit one or more constraints, being the electrical power for heating, the velocity, or the fuse temperature.

In spite of the many changing parameters, the basic model describing the temperatures in the printer remains valid, although several parameter values will change. A deterministic control approach, with extra features to follow the changing operating conditions of the process seems to be a good choice for this problem. A stochastic approach, for example Gaussian processes [14, 15], which neglects the, known, deterministic relations among all variables, has to retrieve all information based on statistical and stochastic properties of the measured variables. An example of the output of such a Gaussian process is shown in Fig. 4.5. Besides an expected value, also the (growing) uncertainty is calculated for increasing prediction horizons. This requires more considerable measurement and calculation time in real-time applications. It can certainly cope with changes in the environment temperature and wear, but it will be too slow to anticipate or counteract the fast changes introduced by printing on different sheets.

Within the class of deterministic control approaches, robust and adaptive control techniques can efficiently cope with time-varying behaviour of the printing system. However, as the largest disturbance is known (print jobs can be predicted), adaptive control is to be preferred over robust control. Robust control without adaptation will be too slow and consequently cannot anticipate fast enough on the known disturbances.

This brings us to the conclusion that adaptive control is most likely the preferred control approach for the control problems formulated for the industrial electro-photography printer. Moreover, any adaptive method that can utilise predicted values of the disturbance and can deal with the many hard constraints is to be preferred.

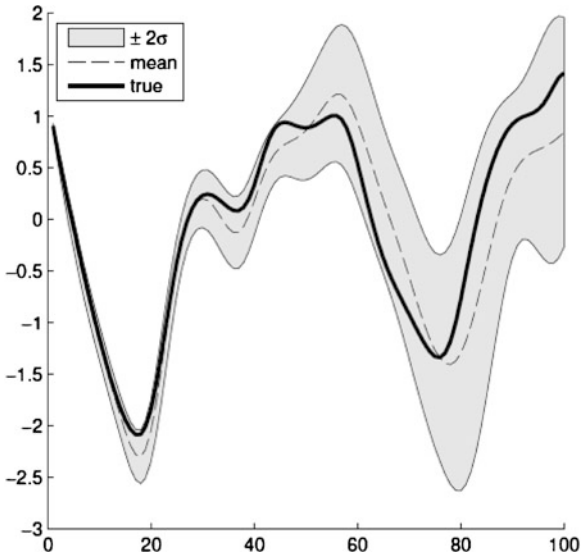

Fig. 4.5 Increasing uncertainty when predicting with a Gaussian process

4.3 Control Design

The major issues that are encountered in the printing system are related to large and fast parameter variations and disturbances (paper size, mass, and humidity) and constraints. These problems influence the performance of the printing system. Good quality means that the fusing temperature should be at a certain desired (print) job-dependent temperature level for all different print jobs. Currently, an industrial PI controller is implemented in the printing system to control the preheating and TTF temperatures. The advantages of the PI controller include a simple structure, easy to design and implement, and there is no need for an accurate model of the process. However, a PI controller has some difficulties in the presence of constraints, it does not adapt itself to changing process behaviour, it is slow in responding to large disturbances, and it does not guarantee optimal performance. In this section, we present the application of three different suitable control strategies to handle these issues.

- *Model Reference Adaptive Control (MRAC)*. MRAC adapts the controller parameters to the operating condition of the process, without explicitly estimating the model or parameters of the process. The same signal is inserted to both the input u of the reference model and to the reference r of the controlled process. Then both outputs are compared which yields the error e. The adaptive mechanism tries to reduce this difference e to zero by adjusting the controller, as presented in Fig. 4.6. When this error is zero, there is no difference between the reaction of the reference model and of the controlled system. So the controlled real process has

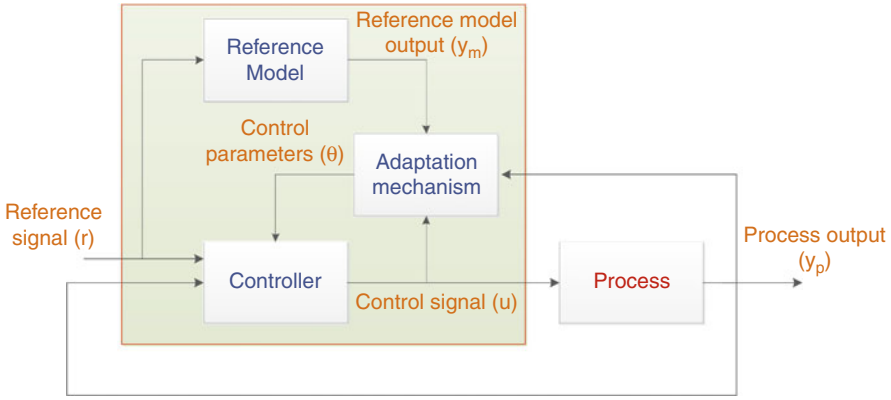

Fig. 4.6 Main structure of Model Reference Adaptive Control (MRAC)

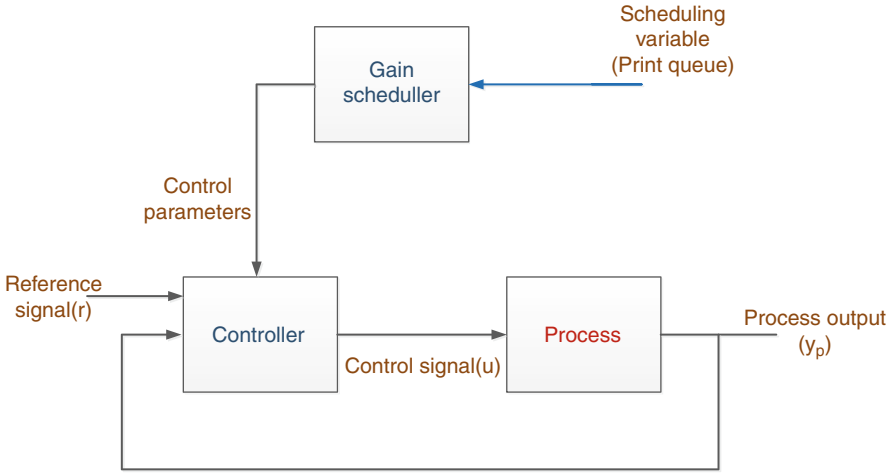

Fig. 4.7 Main structure of gain scheduling robust control

the same behaviour as the selected reference model in spite of disturbances and changing parameters. It is a relative easy control approach with nice performance.

- *Gain scheduling robust control*. The largest disturbance, the print queue, is known in advance. So, an appropriate, pre-designed controller can be calculated for each possible paper sheet in the print queue. When the paper sheet is known, the appropriate controller is taken from the list of available controllers and is applied, see Fig. 4.7.
- *Model Predictive Control (MPC)*. In contrast with the previous methods, MPC uses a prediction horizon. Based on a deterministic model and a to-be-selected input, this technique amounts to predicting the process output. When a criterion

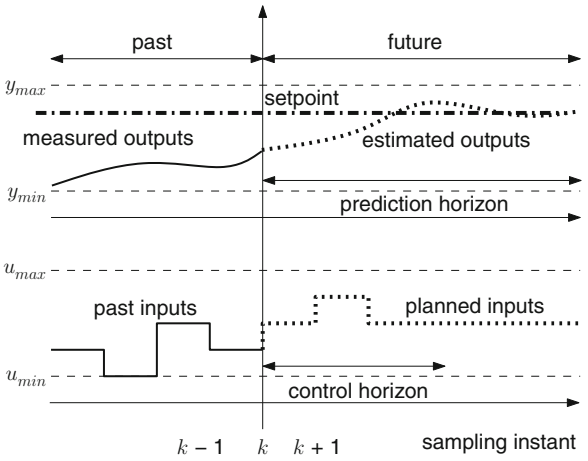

Fig. 4.8 Main structure of model predictive control (MPC)

is utilised that expresses the requirements, even an optimal input sequence can be calculated. As long as the output can be calculated, even when constraints are introduced or known disturbances, still the optimum input sequence can be found. So, MPC can anticipate future sheet characteristics in the print queue and it can take hard constraints explicitly into account. Typically, in MPC the control horizon, the number of implemented control samples, is shorter than the prediction horizon, the number of estimated output samples. The basic idea of MPC is depicted in Fig. 4.8. The lower plot represents the selected inputs (dotted line), while the upper plot represents the calculated output based on these selected inputs. The inputs are selected such that a cost function is minimised over the receding prediction horizon N. A typical cost function assumes the form

$$\mathscr{J}_k(u) = \sum_{i=k+1}^{k+N} \Big((y_{\text{ref}}(i) - y(i))^\top Q_i (y_{\text{ref}}(i) - y(i)) + u(i)^\top R_i u(i) \Big),$$

where y_{ref} denotes the reference variable (e.g. desired temperature), y is the controlled variable (e.g. measured preheating and TTF temperatures), k represents the time instant, Q_i weighting coefficient reflecting the relative importance of the output y, and R_i is a weighting coefficient penalising relative big changes in the input u.

Each control strategy will be shortly described with emphasis on its ability to adapt itself to the disturbances and parameter changes introduced by the different paper sheets in the print queue. The theory behind these methods is explained in the references. After the discussion of these three control approaches, several examples show the characteristics of these controllers for the professional printer example.

4.3.1 Model Reference Adaptive Control

An adaptive controller modifies a control law so as to cope with the time-varying or uncertain parameters of the system being controlled [1, 3]. MRAC is one of the approaches for adaptive control. Model Reference Adaptive Control (MRAC) was first introduced by Whitacker in 1958. Over the past decades, various MRAC methods have been investigated. The majority of MRAC methods may be classified as direct, indirect, or a combination of these. Indirect adaptive control methods are based on the identification of unknown plant parameters and define control schemes derived from the parameter estimates. Parameter identification techniques such as recursive least-squares and neural networks have been used in indirect adaptive control methods. On the other hand, direct adaptive control methods directly adjust control parameters to account for system uncertainties without identifying unknown plant parameters explicitly. Since the printing system has a fast-varying parameters, the adaptation phase has to be as short as possible. Therefore, in this section we focus on direct adaptive control.

The basic structure of a direct MRAC scheme is shown in Fig. 4.6. MRAC schemes aim to reduce the tracking error $e_1 = y_p - y_m$ between the plant output y_p and the output of the reference model y_m. A stable reference model is designed to achieve a desired control performance. The closed-loop system consists of an ordinary control configuration with a feedback control law that contains the plant and a controller $C(\theta)$ and an adjustment mechanism that optimally adjusts the controller parameters $\theta(t)$ in real-time to force the controlled plant to follow the reference-model output. The design procedure involves the use of a wide class of adaptive laws that include least-squares, gradient, and SPR-Lyapunov design approaches [25, 28].

Adaptive control has been successfully implemented in several applications [1,3]. However, the possible high-gain control for fast adaptation is an issue. In some applications, like the professional electro-photography printers, fast adaptation is required to improve tracking performance when a system is subject to large uncertainties. In this case, a large adaptation gain must be used to reduce the tracking error rapidly. However, there typically exists a balance between stability and speed of adaptation. A fast adaptation gain results in high-frequency oscillations, which can excite unmodelled dynamics that could adversely affect the stability of an MRAC system. On the other hand, small adaptation gains will result in an unacceptably slow response.

In this section, we address two different methods to improve the convergence of MRAC, namely, using a non-linearly varying adaptation gain and using multiple adaptation gains with a new adaptation law.

In [8], we have proposed a non-linear time-varying adaptation gain. The design does not require any knowledge of the parameters of the system. To improve the system performance, the adaptation gain should be chosen as a function of the controller parameters error. However, the optimal controller parameters depend on the process parameters, which are usually unknown. The error between the outputs

of the process and of the reference model gives a useful indication of the controller parameter errors. Hence, we propose an adaptation gain as a function of the output error instead of controller parameter error.

Besides state feedback, we have also derived adaptation laws on the basis of output feedback in [7], but those will not be discussed here.

Consider a linear time-varying system given by

$$\begin{aligned} \dot{x}(t) &= A_p(t)x(t) + B_p(t)u(t), \\ y(t) &= C_p x(t), \end{aligned} \tag{4.13}$$

where $x(t)$ is the state vector of the plant (professional printer), $y(t)$ is the plant output, and $u(t)$ denotes the plant input. For the professional printer, these variables are the ones that are defined in Sect. 4.2.2. The matrices $A_p(t)$, $B_p(t)$, C_p are the state space realisation of the printing system model (4.6), which are assumed to be time varying.

Suppose that the stable reference model is given by

$$\begin{aligned} \dot{x}_m(t) &= A_m x_m(t) + B_m r(t), \\ y_m(t) &= C_m x_m(t), \end{aligned} \tag{4.14}$$

where $r(t)$ is a reference input signal, $x_m(t)$ is the state vector of the reference model, $y_m(t)$ is the reference output, A_m, B_m, and C_m are the state space matrices of the reference system. The reference model is chosen to represent a desired performance of the closed-loop system.

It can be shown that with the state feedback control law

$$u(t) = K_{\mathrm{FF}}(t)r(t) + K_{\mathrm{FB}}^{\top}(t)x(t), \tag{4.15}$$

which is written in a compact form as

$$u(t) = \theta^{\top}(t)V(t), \tag{4.16}$$

where $\theta(t) = col(K_{\mathrm{FF}}(t),\ K_{\mathrm{FB}}(t)) \in \mathbb{R}^{1+n}$ denotes the controller parameter vector, n represents the number of states, and $V(t) = col(r(t),\ x(t)) \in \mathbb{R}^{n+1}$ is the regressor vector.

An adaptive control law exists that defines the evolution of $\theta(t)$ and that forces the difference $e(t) = x(t) - x_m(t)$ to zero. So ultimately the state of the process $x(t)$ and the state of the reference model $x_m(t)$ will become the same. The process behaves like the (desired) reference model in spite of disturbances and parameter uncertainty. For time-invariant models (4.13) and (4.14), the closed-loop system is asymptotically stable ($e \to 0$ as $t \to \infty$) using the control law (4.16) and the update law

$$\dot{\hat{\theta}} = \dot{\theta} = -\Gamma w B_I^{\top} W e, \tag{4.17}$$

with $B_I = [0 \quad \cdots \quad 0 \quad 1]^\top \in \mathbb{R}^n$ and $W \succ 0$ a positive definite matrix, which satisfies $A_m^\top W + W A_m \prec 0$. The speed of convergence is determined by a gain Γ. This adaptation gain Γ determines the rate at which the controller parameter will converge to steady-state values. Moreover, the adaptation gain influences the performance of the system. Hence, the adaptation gain should be properly chosen. A high adaptation gain may lead to badly damped behaviour, while a low adaptation gain will lead to an unacceptable slow response.

A new MRAC state feedback design is introduced based on a non-linear adaptation gain. The adaptation gain Γ is chosen as a function of the error e such that if the error is large, the adaptation gain Γ will be large. This implies that the controller will adapt its parameters faster and thus a faster convergence of the error is achieved.

Let the adaptation gain be

$$\Gamma = \gamma_0 + \gamma_1 e^\top P e, \quad \gamma_0 > 0, \quad \gamma_1 > 0, \quad P \succ 0, \quad \text{therefore} \quad \Gamma > 0. \tag{4.18}$$

Using the state feedback control law (4.16), the adaptation law (4.17), and the non-linear adaptation gain (4.18), the closed-loop system is still asymptotically stable. Note that γ_0 and γ_1 are design parameters. The non-linear adaptation gain (4.18) is more generic than the standard MRAC with a constant adaptation gain ($\gamma_1 = 0$). It will show faster convergence without sacrificing stability.

A further performance improvement of MRAC is obtained in [10], where a novel adaptation law is introduced for both state and output feedback. Unlike the standard MRAC, which uses a single constant adaptation gain, multiple adaptation gains are employed in this approach. The error dynamics, which are composed of the output tracking error and the controller parameter estimation error, are first represented by a Takagi-Sugeno (T-S) model [26]. The T-S model is considered as an exponentially stable system perturbed by an external disturbance. Therefore, the adaptive control problem is formulated as minimising the $\mathscr{L}_2$ gain. By this formulation, the optimal adaptation gains are obtained by solving a linear matrix inequality (LMI) problem [2].

In this approach, a new adaptation law is defined as

$$\dot{\theta}(t) = \sum_{i=1}^{L} h_i(V(t)) \left(\Gamma_i e(t) + \beta_i \theta(t)\right) \tag{4.19}$$

where, for all i, $h_i : \mathbb{R}^{n+1} \to \mathbb{R}$ is such that $h_i(V(t)) \geq 0$ and $\sum_{i=1}^{L} h_i(V(t)) = 1$ for all $V(t) \in \mathbb{R}^{n+1}$. Here, L represents the number of subsystems and Γ_i and β_i are adaptation design variables.

Using the state feedback control law (4.16) with the adaptation law (4.19), an LMI feasibility problem is formulated such that the error dynamics of the closed-loop system is guaranteed to be asymptotically stable.

The key advantage of this approach is to select in real-time the best adaptation gain from an a priori designed set of adaptation gains. The adaptation gain is selected based on the operating point of the system states. Consequently, the adaptation transients have been considerably improved. For more details about this approach, interested readers are referred to [7].

4.3.2 Gain Scheduling Robust Control

The Takagi-Sugeno (T-S) model has been widely used in various applications since it can efficiently model and control complex non-linear systems. A T-S model, which was introduced in [26], is composed of a weighted sum of local linear models. A T-S model approximates a non-linear system and the weights in the T-S model depend on the operating point of the non-linear system. According to the universal approximation theorem [29], a T-S model can approximate a non-linear system arbitrarily well. Recently, T-S model-based controllers have been applied to stabilise non-linear systems [4, 27].

The T-S model is formally presented as a weighted average of several linear models through weighting functions. The T-S model is defined as:

$$\Sigma : \begin{cases} \dot{x}(t) = \sum\limits_{i=1}^{L} h_i(z(t)) \left(A_i\, x(t) + B_i\, u(t)\right), \\ y(t) = \sum\limits_{i=1}^{L} h_i(z(t))\, C_i\, x(t), \end{cases} \tag{4.20}$$

for $i = 1, \ldots, L$, where $A_i \in \mathbb{R}^{n \times n}$, $B_i \in \mathbb{R}^{n \times m}$, $C_i \in \mathbb{R}^{p \times n}$, and L denotes the number of linear models. Note that all matrices have identical dimensions independent of their index i. $h_i(z(t)) \geq 0$ for $i = 1, \ldots, L$, $\sum_{i=1}^{L} h_i(z(t)) = 1$, and $z(t)$ is a triggering (scheduling) variable, which is usually dependent on the current value of the system state $x(t)$. $z(t) \in \mathbb{R}^n$ is the variable that decides about the operating point. In our professional electro-photography printer, $z(t)$ represents the known print queue.

The structure of the T-S model has led to the design of a feedback controller for each local model, which are further combined into a single overall controller by a weighted combination as follows

$$u(t) = \sum_{j=1}^{L} h_j(z(t)) K_j x(t). \tag{4.21}$$

Here, K_j are the controller gains for $j = 1, \ldots, L$ and the weighting functions $h_j(z(t))$, for $j = 1, \ldots, L$, are the same as in (4.20).

The T-S model structure has been used as a feasible approach to capture the dynamic characteristics of printing system under different operating conditions. The approximation error (or misfit) between the original non-linear printing system

and the T-S model is known as the *consequence uncertainty*. Designing a stabilising controller based on the T-S model may not guarantee the stability of the original non-linear system under such a controller.

In [9, 11], we have addressed the robust control problem of an electro-photography printing system, using an $\mathscr{L}_2$ state and output feedback controller. The non-linear printing system is approximated by a Takagi-Sugeno (T-S) model. A robust control technique is proposed to cope with the effect of the approximation error between the non-linear model of the printing system and the approximating T-S model. A sufficient condition is derived to ensure robust stability of an $\mathscr{L}_2$ state and output feedback controller with a guaranteed disturbance attenuation level. A technique based on a parameterised Lyapunov function is employed in our approach. The control problem is formulated in terms of a linear matrix inequality for which efficient optimisation solvers are used to test feasibility. In this framework, we utilise the known paper characteristics of the print queue as triggering (scheduling) variable. So, for each paper mass we can select the best fitted controller. The implementation of this technique for the printing system is explained in more detail in Sect. 4.4.

4.3.3 Model Predictive Control

An important research challenge is to design a run-time adaptive system that maintains a high level of economic performance, i.e. to maximise throughput for the printer, under non-linear dynamic behaviour and changing, partly known operating conditions. To deliver high performance, the system should adapt itself in run-time, based on the operating conditions and constraints. In our case, the adaptation is mainly related to changes in the media type (print queue). Model predictive control (MPC) is a good choice to control the behaviour of printers, because it can deal in an optimal way with hard constraints and available information of the print queue [21]. MPC makes use of a model of the system to compute the optimal inputs. Since the paper properties directly influence the system dynamics, different models should be used in control for different paper types, when heating up the system and printing. A non-linear parameter-varying model of the system could capture all the dynamics of the process. Several approaches have been proposed in literature to deal with model predictive control for linear parameter-varying systems e.g. [19, 31]. When large transitions between setpoints are required, as in the case of changing operating points, tracking control of a constrained non-linear system is a challenging problem [12, 22].

Systems with input-induced non-linearities [5] are a special type of non-linear systems. They are a class of input-dependent non-linear systems. Some of the inputs are considered to be more active in the dynamic behaviour of the system than others. If inputs and known disturbances that induce non-linear behaviour are constant for some period, the system can be approximated by a linear one in those periods. Therefore, the input is divided into two components $u(k) = col(u_d(k), u_l(k))$, where

$u_d := col(v,d)$ and $u_l := col(P_{\text{pre}}, P_{\text{TTF}})$. According to the printing system heat model (4.6), with u_d constant, the system will be linear with respect to u_l.

A good control approach, which assures both maximum throughput and the high quality of the system, is based on a non-linear dynamic input-dependent predictive controller. It will be presented in this section. The controller has to track a variable target, while respecting hard constraints of the plant, coping with the uncertainties due to modelling errors and partly known disturbances. Based on the printing system model, we formulate the control problem into centralised and decomposed strategies.

4.3.3.1 Centralised Control Strategy

The objective is to design a controller which can assure maximum throughput while keeping the print quality within constraints under all operating conditions. Knowing a few seconds in advance what type of paper will come in the fusing point, the question is how to determine the optimal heating strategy for the printing process in cold start and warm process. This information can be used in feedforward to obtain a better performance of the system. The printer needs to be heated up to a certain temperature to make sure that the print quality is not lost, not even for one page. During printing, there may be several switches between different types of paper. Optimising the distribution between P_{pre} and P_{TTF}, v and d, can improve the throughput during switches.

The control scheme will have to adapt itself between several modes, e.g. cold start, warm process, depending on the media type.

Given a non-linear system represented by a discrete-time model:

$$\begin{aligned} x(k+1) &= f(x(k), u(k), \theta(k), w(k)) \\ y(k) &= g(x(k), u(k), \theta(k)) \end{aligned} \tag{4.22}$$

where x is the system state vector, u is the input vector, $\theta(k)$ is the time-varying input-dependent known parameter vector, which represents the known paper properties, w is the unknown disturbance vector, and y is the measured output of the system. The system is subject to hard constraints on x, u, y, and w, as explained in Sect. 4.2.2. The output of the system y contains, beside the measured outputs (T_{pre}, T_{TTF}), the estimated fuse temperature T_{fuse}.

In industrial control systems, the goal is to optimise dynamic plants from an economic point of view. It is required to steer the system along a time-varying target. The controller has to track the target, given the hard constraints of the plant, while considering the uncertainties included in system the modelling and measured and unmeasured disturbances. The time-varying target can be determined based on real-life observations or based on optimisation rules, given some specific criterion.

Since most of the industrial plants are subject to hard constraints, a good solution of the problem can be based on a model predictive formulation.

The model predictive control (MPC) method is conceptually a method for generating feedback control actions for linear and non-linear plants subject to constraints, especially if predictions of the disturbances are available (θ). It is one of the most successful control techniques in process industry [21]. In principle, based on the past inputs and outputs, but also on the future control scenario (the control actions that we intend to apply from the present moment k onwards), at each sample k, the process output y is predicted over a prediction horizon N. A reference trajectory is defined over the prediction horizon, to force the process output to follow a predefined trajectory y_{ref}. This information is used by the controller to provide the optimal control input vector u^*, according to a predefined optimisation cost function. Only the first element of the optimisation will be applied to the process, and the remaining elements of the optimisation will be discarded. The same procedure will be repeated at each sample.

The optimal solution $u^* = col(u_d^*\, u_l^*)$, at time instant k, satisfies:

$$u^* = \arg\min_{u} \sum_{i=1}^{N} [\mathscr{J}(u_d(i), \theta(i)) + \lambda (y(i) - y_{\text{ref}}(u_d(i), \theta(i)))^2] \tag{4.23}$$

such that

$$\begin{aligned} x(0) &= \hat{x}(k) \\ x(i+1) &= f(x(i), u(i), \hat{w}(i), \theta(i)) \\ y(i) &= g(x(i), u(i), \theta(i)) \\ i &\in I_0^{N-1} = \{0, \ldots, N-1\} \\ x(i) &\in \mathrm{X}\ \ u(i) \in \mathrm{U}\ \ y(i) \in \mathrm{Y} \\ \sum_{j=1}^{m_l} u_{l_j}(i) &\leq u_{\max}(k) \\ |u_d(i) - u_d(i-1)| &\leq \overline{u_d}. \end{aligned}$$

A trade-off is being made between the economic performance of the system and output tracking in the cost function using the penalty function λ. The economic performance, e.g. printers with high throughput are desired, is described by $\mathscr{J}(u_d(i), \theta(i))$ (4.12). The output of the system $y(i)$ is forced to follow a desired value $y_{\text{ref}}(u_d(i), \theta(i)))$ (e.g. required performance criterion for print quality computed based on knowledge of known input u_d and estimated θ) for each time instant, $i \in I_0^{N-1}$, with N the prediction horizon. For λ small, output tracking does not play an important part in the cost function, while for increased values of λ output tracking becomes dominant. Over the prediction horizon N, the values of the system parameters $\theta(i)$ are known and they can change each sample, $\theta(i) \in \Gamma$. The estimated values of disturbances are between bounds $\hat{w} \in \Phi$. The non-linear optimisation is performed in the presence of hard constraints. The sum of u_l inputs

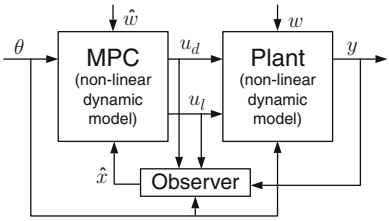

Fig. 4.9 Centralised control scheme of the system

is limited any moment in time by a time-varying maximum $u_{\max}$ (e.g. a physical limitation of the available power). The variation in $u_{\max}$ is random (no model available) but bounded. Since no prediction can be made for the future, $u_{\max}$ is assumed to be constant and equal to the last known value. Due to some physical limitations of the system, an upper bound $\overline{u_d}$ of the rate of change in u_d input is taken into account in the problem formulation. A piece-wise linear observer is built to estimate the system states $\hat{x}$, since not all the states are measurable. It uses a linearised system model around $u_d(k)$ computed in the previous step and known $\theta(k)$.

The control scheme of the process, including the controller and the observer, is shown in Fig. 4.9.

To assess the stability of the system, a control Lyapunov function (CLF) can be derived and expressed in the optimisation problem [18, 24].

As it was mentioned in Sect. 4.2.2, an interesting challenge for printers is the cold start. To maximise the productivity of the printer, it is important to determine the optimal heating strategy when the printing process can start. The machine needs to be heated up as fast as possible to achieve print quality for the first page too. After the printing process starts, the speed and the distance between sheets need to be adjusted, until a steady state is reached. The process is highly non-linear and influenced by several disturbances during cold start. All the dynamics are changing, and in case of shortage in power, the power distribution plays an important role in determining the system performance.

For the given input-dependent model of the system (4.22), the switching between printing modes (cold start, warm process), translates into adaptation of the control scheme to a new set of parameters θ, e.g. cold start without paper $\theta = \theta_1$, warm process with different types of paper $\theta = \theta_i$, with the index i represent the type of paper.

4.3.3.2 Decomposed Control Strategy

The printing system (4.6) is represented by an input-induced non-linear dynamic model, as explained in Sect. 4.3.3. For the centralised formulation, all four inputs are computed dynamically using the non-linear dynamic model of the printing system. However, here the non-linear dynamics of the system could be divided into

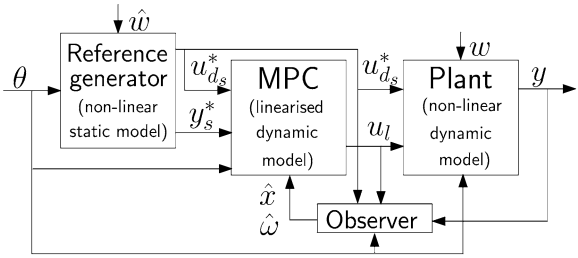

Fig. 4.10 Decomposed control scheme of the system

a non-linear static model and a linearised dynamic model. Therefore, the control system can be decomposed into two levels to apply a second control approach, as shown in Fig. 4.10.

- *Reference generator*. This is a non-linear feedforward optimisation scheme used in run-time for reference generation. It uses the static non-linear model of the system and takes into account the operating conditions, the system constraints and known parameters for N samples. This static optimisation assures maximum throughput in steady-state. The optimal steady-state solution for $(u^*_{d_s}, u^*_{l_s}, y^*_s)$ is determined. The used scheme decouples the u_d input, which makes the printing system linear for the feedback control loop (MPC level).
- *MPC*. In this level, setpoint tracking and print quality satisfaction (robustness against modelling errors and unmeasured disturbances) are achieved using a linear model predictive controller (MPC) formulation. The design of the MPC employs a linearised model of the system around the optimal $u^*_{d_s}$ obtained from the static optimisation level. To obtain off-set free tracking with the MPC, i.e. zero steady-state error, a disturbance filter is used [21], to estimate and predict the mismatch between measured and predicted outputs. An observer is designed to estimate the system state $\hat{x}$ and the disturbances $\hat{\omega}$.

This control strategy requires less computation time compared to the control scheme described in Sect. 4.3.3.1. That makes it attractive for real-time implementation for the printing system. However, transient performance cannot be guaranteed when changing the operating conditions because part of the inputs are obtained based on static optimisation.

4.4 Professional Electro-Photography Printing Systems under Control

In this section, we present the implementation of the three control schemes described in Sect. 4.3 to the printing system. We also compare between the performance of both these control schemes and the industrial PI controller that is current used in the printer. To have a fair comparison, the PI controller is a well-tuned industrial controller.

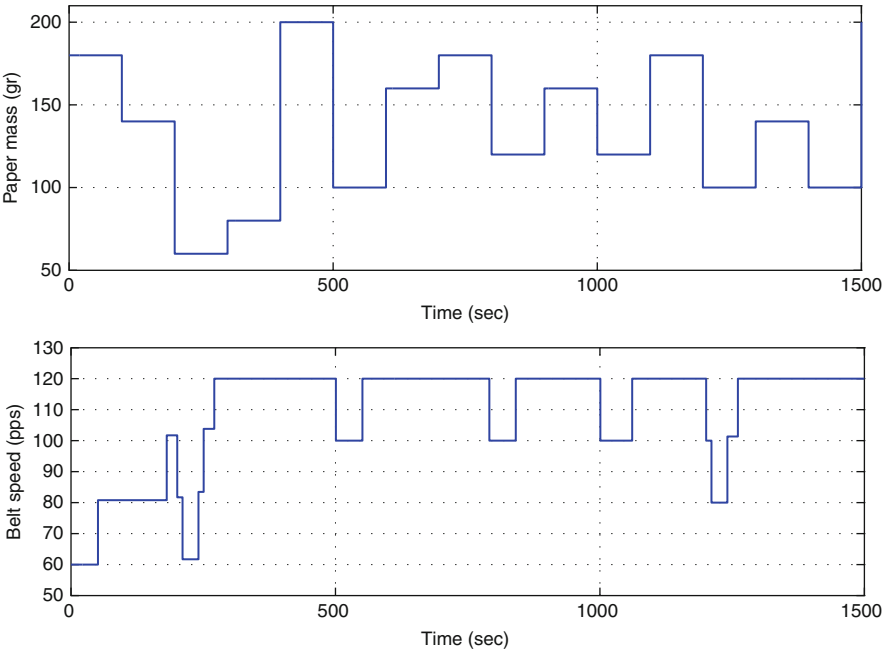

Fig. 4.11 The variation of the paper mass and the transfer belt speed

4.4.1 Model Reference Adaptive Control

Based on the printer characteristics, MRAC is suggested to control the fuse temperature. The objective is to design a controller to keep both the print quality and the productivity as good as possible. Here, we present a comparison of the tracking control results of the existing industrial PI controller and the proposed MRAC approaches.

In the printing system (4.6), the control input is $u(t) = col(P_{\text{pre}}(t), P_{\text{TTF}}(t))$, and the measured output is $y(t) = col(T_{\text{pre}}(t), T_{\text{fuse}}(t))$. Several parameters of the printing system are time-varying since these parameters depend on the different printing jobs, while other parameters are unknown. As shown in Fig. 4.11 the paper mass and the speed are varied to simulate the parameter variations.

To achieve a short transient time with little overshoot, we choose the reference models for the preheater and the TTF as

$$A_{r_{\text{pre}}} = -0.5, \quad B_{r_{\text{pre}}} = 0.5, \quad C_{r_{\text{pre}}} = 1,$$

$$A_{r_{\text{TTF}}} = \begin{bmatrix} 0 & 1 & 0 \\ 0 & 0 & 1 \\ -0.125 & -0.75 & -1.5 \end{bmatrix}, \quad B_{r_{\text{pre}}} = \begin{bmatrix} 0 \\ 0 \\ 0.125 \end{bmatrix}, \quad C_{r_{\text{pre}}} = \begin{bmatrix} 1 & 0 & 0 \end{bmatrix}.$$

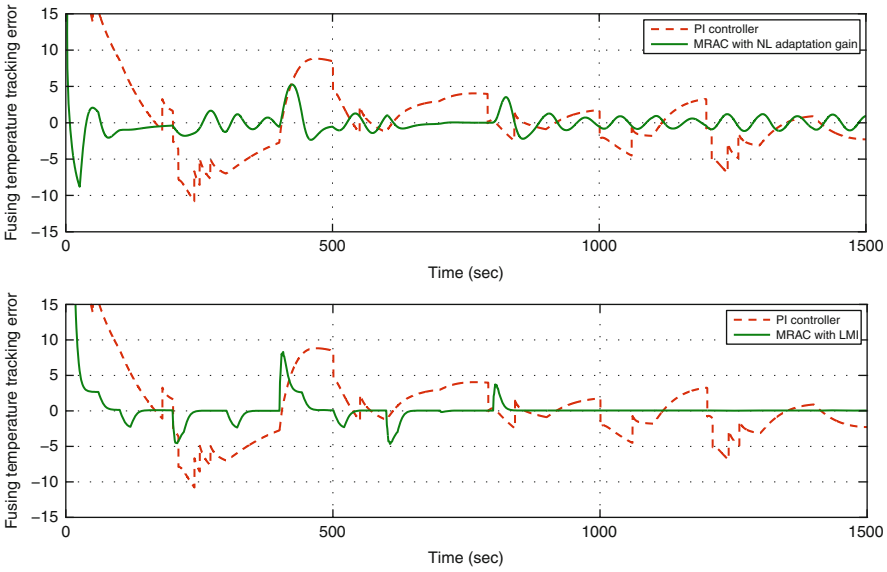

Fig. 4.12 Fusing temperature tracking error

The designer is free to choose the reference model according to the desired closed-loop performance.

Since the fusing temperature depends on the preheating and the TTF temperature, we apply MRAC with the non-linear adaptation gain to control both the preheating and TTF temperature. We also implement the adaptive control law with the multiple adaptation law. To construct the T-S model that approximates the error dynamics, we assume that $V_{\text{pre}} \in [\mathcal{N}_{\min}, \mathcal{N}_{\max}]$ and $V_{\text{TTF}} \in [\mathcal{M}_{\min}, \mathcal{M}_{\max}]$. We choose

$$\mathcal{N}_{\min} = col(50,50), \quad \mathcal{N}_{\max} = col(100,100),$$

$$\mathcal{M}_{\min} = col(0,0,0,0), \quad \mathcal{M}_{\max} = col(100,100,1000,1000).$$

The triangle shape weighting functions are adopted for this approach.

Figure 4.12 compares the fusing temperature tracking error of the existing industrial PI controller, the MRAC with a non-linear adaptation gain, and the MRAC with multiple adaptation gains. As depicted, the tracking performance of both MRAC schemes are better than that of the PI controller in the presence of large parameter variations. Figure 4.13 presents the preheating temperature tracking of different temperature levels with paper mass variations. These simulation results illustrate that the proposed MRAC schemes can efficiently improve the performance of the printing system in the presence of large parameter variations.

Using MRAC with a non-linear adaptation gain guarantees a faster convergence of the tracking error to zero but it does not guarantee the convergence of the controller parameters to the optimal value. On the other hand, employing the adaptive

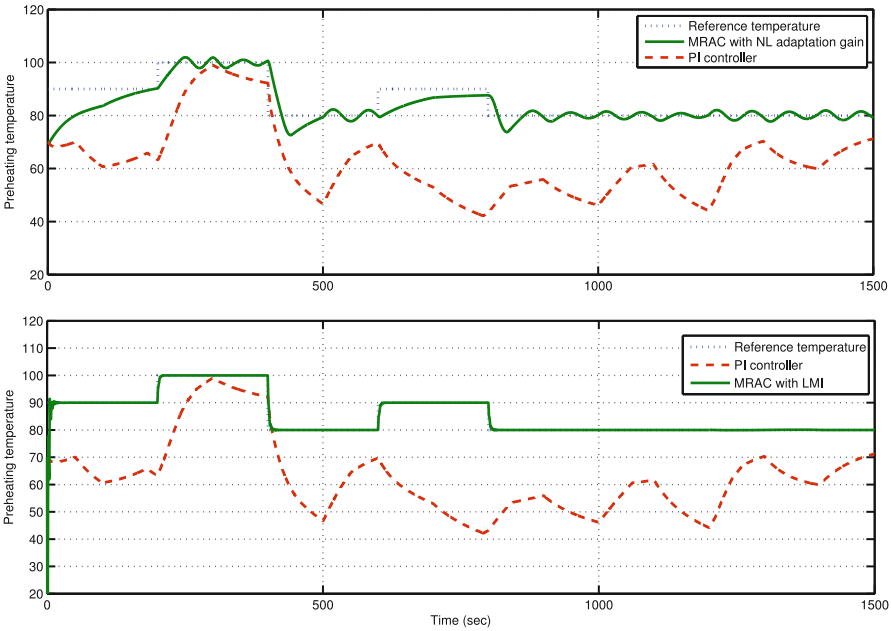

Fig. 4.13 Preheating temperature tracking control comparison

law with multiple adaptation gains yields convergence of both the tracking and the controller parameters errors. Thanks to the representation of the augmented error as a T-S model, the adaptive problem is formulated as an LMI feasibility problem and, therefore, the optimal adaptation gains are obtained. That explains the better performance of the MRAC with multiple adaptation gains compared to the MRAC with the non-linear adaptation gain.

4.4.2 Gain Scheduling Robust Control

In this section, we present the implementation of the robust control scheme to the electro-photography printing system and the comparison between the performance of both the proposed robust control scheme and the existing industrial PI controller.

Given the knowledge of the paper mass m and the belt speed v, the printing system dynamics are approximated with a T-S model. Note that the choice of the number of the sub-models L depends on the available knowledge about the operating conditions of the system. A large number of sub-models will result in a small approximation error with high complexity and vice versa. There is always a trade-off between complexity and accuracy. Therefore, the T-S model which approximates the printing system (4.6) is represented using the following set of nine linearised models:

$$\dot{x}(t) = \sum_{i=1}^{9} h_i(z(t)) \left(A_i x(t) + B_i u(t) + E\hat{d}(t)\right),$$
$$y(t) = \sum_{i=1}^{9} h_i(z(t)) C_i x(t). \tag{4.24}$$

We choose the following nine working regions Ri to describe the dynamics of the printing system:

R1: $m \leq 80$ and $v \leq 60$,
R2: $m \leq 80$ and $60 \leq v \leq 90$,
R3: $m \leq 80$ and $90 \leq v \leq 120$,
R4: $80 \leq m \leq 140$ and $v \leq 60$,
R5: $80 \leq m \leq 140$ and $60 \leq v \leq 90$,
R6: $80 \leq m \leq 140$ and $90 \leq v \leq 120$,
R7: $140 \leq m \leq 200$ and $v \leq 60$,
R8: $140 \leq m \leq 200$ and $60 \leq v \leq 90$,
R9: $140 \leq m \leq 200$ and $90 \leq v \leq 120$,

where $x(t) = \left[T_{\text{pre}}\ T_{\text{TTF}}\ T_{\text{roller}}\ T_{\text{slow}}\right]^{\top}$, $u(t) = \begin{bmatrix} P_{\text{pre}}(t) \\ P_{\text{TTF}}(t) \end{bmatrix}$, $\hat{d}(t) = T_{\text{env}}(t)$ is the environment temperature, $y(t) = \begin{bmatrix} T_{\text{pre}}(t) \\ T_{\text{TTF}}(t) \end{bmatrix}$, and the triggering variables $z(t) := col(m, v)$.

After several iterations using the LMI optimisation toolbox in MATLAB [23], we found the optimal controller parameters that guarantee an $\mathscr{L}_2$ gain is 0.5. As shown in Fig. 4.14, the external disturbance $\hat{d}(t)$ (environment temperature) is assumed to vary between 15 and 30 °C. The variation of the paper mass and the belt speed is depicted in Fig. 4.11. To achieve a good print quality, the T_{TTF} and T_{pre} should be kept at a certain desired setpoint. T_{TTF} and T_{pre} are used to estimate the fusing temperature. Figure 4.15 shows the fusing temperature tracking error comparison. As shown, the tracking performance of the robust controller is better than the PI controller in the presence of the parameter variations and the external disturbance. Figure 4.16 shows the preheating temperature tracking of different temperature levels with paper mass variations. The simulation results show that the observer-based $\mathscr{L}_2$ controller has considerably improved the print quality with relatively large external disturbances while the desired performance is still being achieved.

4.4.3 Model Predictive Control

In this section, the control performance will be analysed of both the centralised and the decomposed MPC controllers. These controllers must be robust with respect to

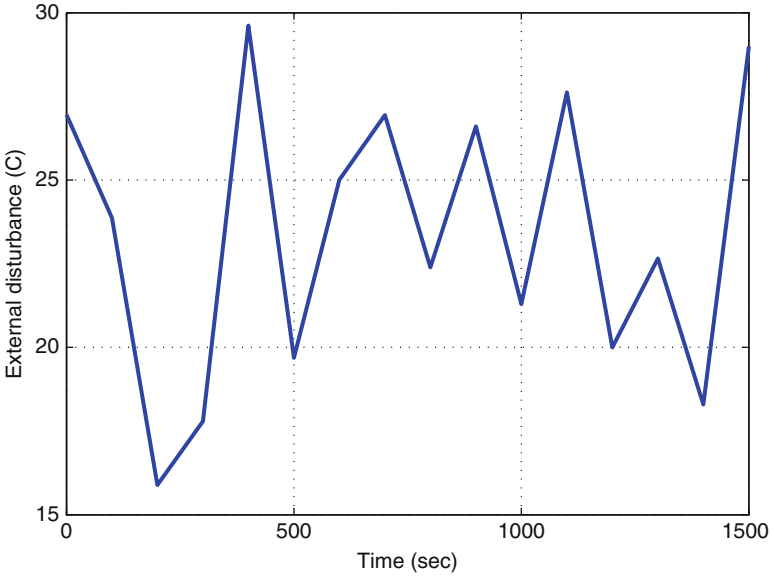

Fig. 4.14 The external disturbance $\hat{d}(t)$

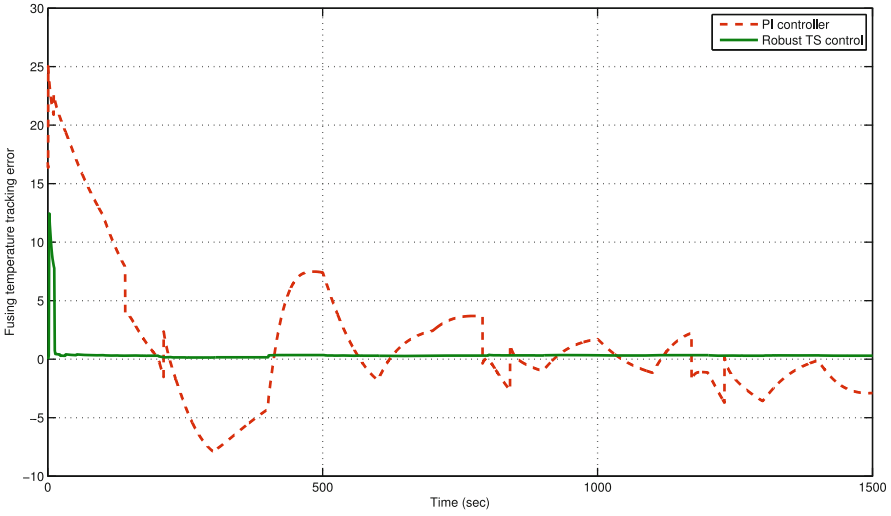

Fig. 4.15 Fusing temperature tracking error

variation in media/print queue (mass of the paper m, initial temperature of the paper T_{init}, dimensions l and b, specific heat capacity c), environment temperature T_{env} and variations in constraints, such as maximum available power.

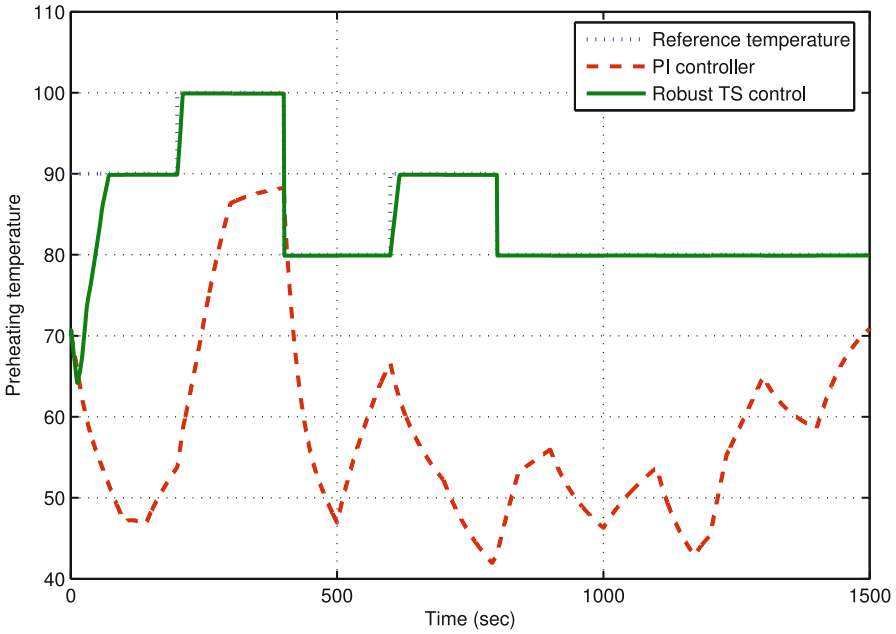

Fig. 4.16 Preheating temperature tracking control comparison

For the warm process, we will illustrate the results obtained for variation in paper mass (since this influences system dynamics the most) and variation in maximum available power (one of the constraints that may not be violated under any circumstances).

4.4.3.1 Centralised Model Predictive Control

The centralised (non-linear) dynamic predictive controller has been designed based on the system characteristics and a known print queue. Since we know in advance what kind of paper will enter the fusing point, we can use this information. The discrete model, to compute the prediction of the output over the prediction horizon, has been obtained from (4.6), (4.7), and (4.12) by discretising with sampling time $T_s = 0.5$ s.

A prediction horizon of $N = 6$ (3 s in advance) is used and for every sample the paper characteristics $\theta(i), i \in I_0^{N-1}$ can be different. In the cost function of the non-linear dynamic controller (4.23) the economic performance is the productivity (4.12) and the output tracking is represented by the fusing temperature T_{fuse} and the preheater temperature T_{pre}. The fusing temperature T_{fuse} has the highest priority $\lambda_1 = 10$ and the preheater temperature T_{pre} has the lowest priority $\lambda_2 = 0.9$, since it is the slowest part of the system and in many cases it can be compensated with

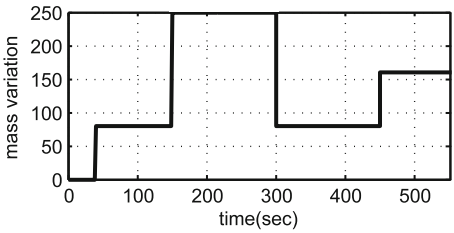

Fig. 4.17 Mass of the paper variation

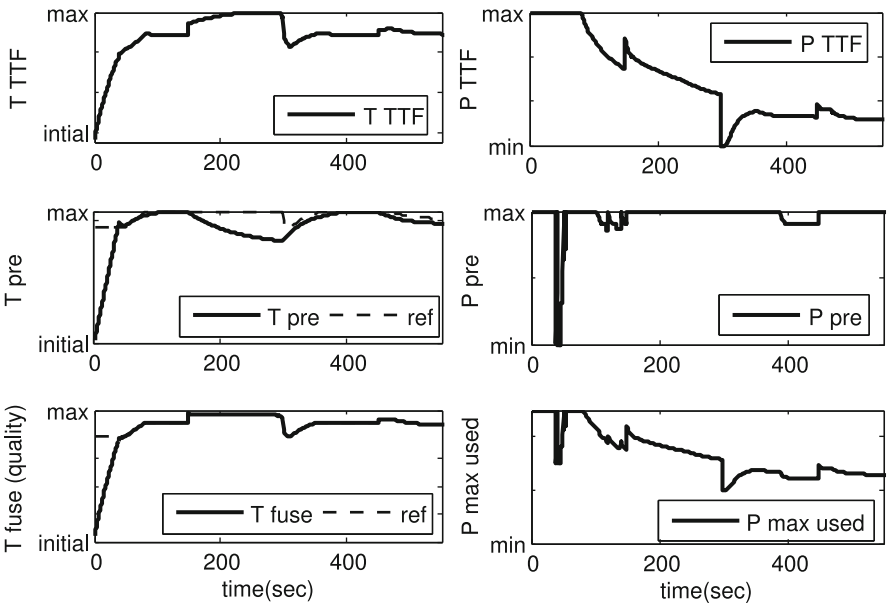

Fig. 4.18 MPC-centralised: Controlled temperatures in the presence of mass variation

the T_{TTF} to obtain the required T_{fuse}. The optimisation is performed on-line and each sample all four inputs $(v, d, P_{\text{pre}}, P_{\text{TTF}})$ are calculated to keep the system's economic performance at a maximum. They are sent directly to the system and at the next sample, based on the output measurements, new inputs will be computed on-line. The unknown disturbances w are some of the paper properties and environment temperature. The outputs y are the measured temperatures of the preheater T_{pre}, the TTF belt T_{TTF}, and the estimated fuse (quality) temperature T_{fuse}.

At cold start, the controller has to determine the initial point, when the printing can start and to heat the printer components as fast as possible to that point. Once $T_{\text{fuse}} \approx T_{\text{ref}}(u_d, \theta)$, determined based on the characteristics of the first sheet and speed, the printing process can start.

Figure 4.17 presents the variation in the mass of the paper between the minimum and maximum allowed $(m_{\min}, m_{\max})[\text{gr}/\text{m}^2]$. For the first seconds, the mass of the paper is zero because the printer is not warm enough, therefore the printing process cannot start yet. Figure 4.18 presents the optimal variation of temperatures inside

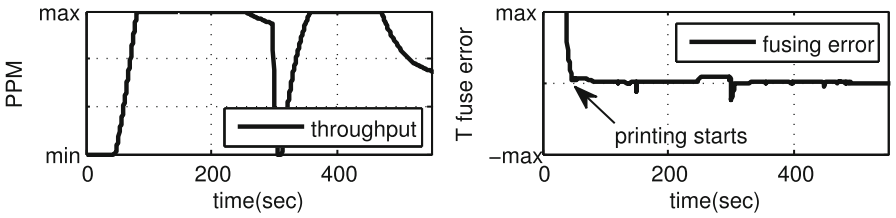

Fig. 4.19 MPC-centralised: Productivity and fuse error for mass variation

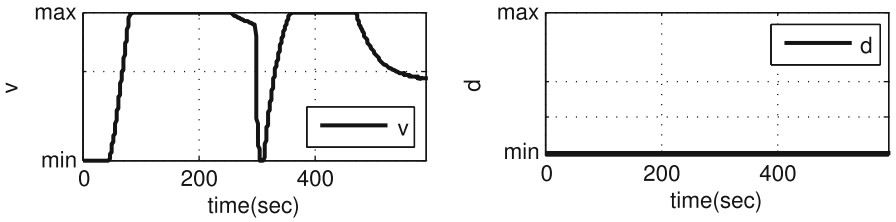

Fig. 4.20 MPC-centralised: Belt speed and distance between sheets for mass variation

Fig. 4.21 Maximum available power variation

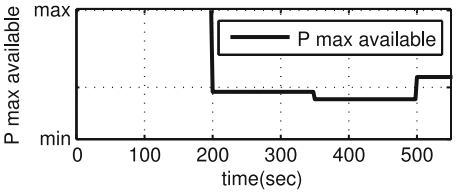

the printer, obtained for the considered case in Fig. 4.17. The plots on the left hand side represent the controlled output of the system to the reference (T_{TTF}, T_{pre}, T_{fuse}). While the plots on the right hand side show the control actions for the TTF and preheater (P_{TTF}, P_{pre}) as well as the maximum used power by the two elements. The references for T_{pre} and T_{fuse} are obtained based on the speed of the engine v and paper properties θ, $y_{\text{ref}}(v, \theta(k))$. The throughput and the error in the fusing point are shown in Fig. 4.19. The throughput has been adjusted on-line according to the available resources. Different combinations of engine speed and distance between sheets can give the same throughput. Since variation in speed of the engine is more energy efficient than adjusting the distance between sheets, the distance between sheets is minimum and speed is varied all the time, see Fig. 4.20. The error in the fuse is very small and remains, after the cold start, always within its bounds.

The maximum available power is an important constraint. The controller must take into account this hard constraint and obtain a feasible, yet optimal, solution. Figure 4.21 presents random steps in the maximum available power. The control scheme knows this maximum, but no prediction is possible. Figures 4.22–4.24 show the robustness and performance of the control scheme with respect to the maximum available power. The fuse quality error in this case is almost zero.

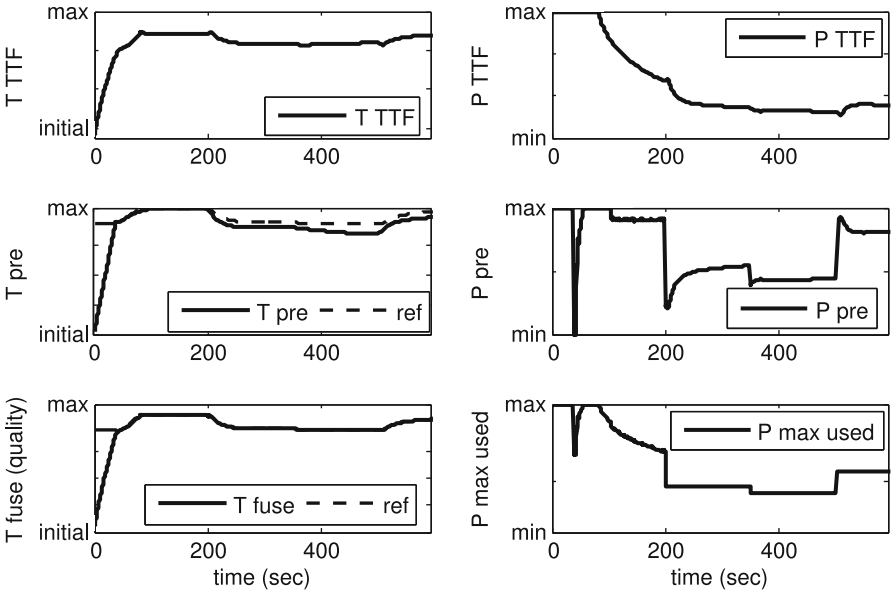

Fig. 4.22 MPC-centralised: Temperatures in presence of $P_{\max}$ variation

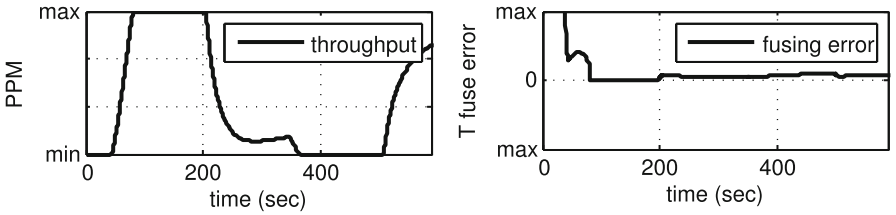

Fig. 4.23 MPC-centralised: Productivity and fuse error in presence of $P_{\max}$ variation

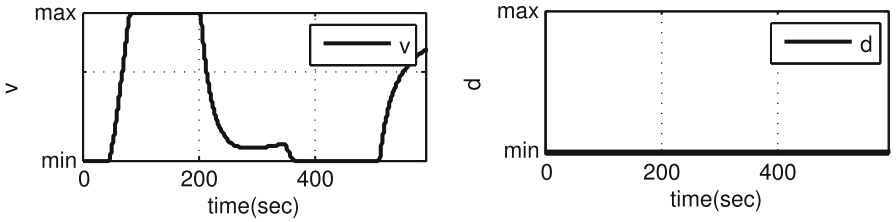

Fig. 4.24 MPC-centralised: Belt speed and distance between sheets with $P_{\max}$ variation

The disadvantage of this control scheme is that the computation time is large for large prediction horizons. Then, the optimal value of the input u cannot be calculated in real-time. For the same considered case studies, the performance of the decomposed MPC will be analysed in the next section.

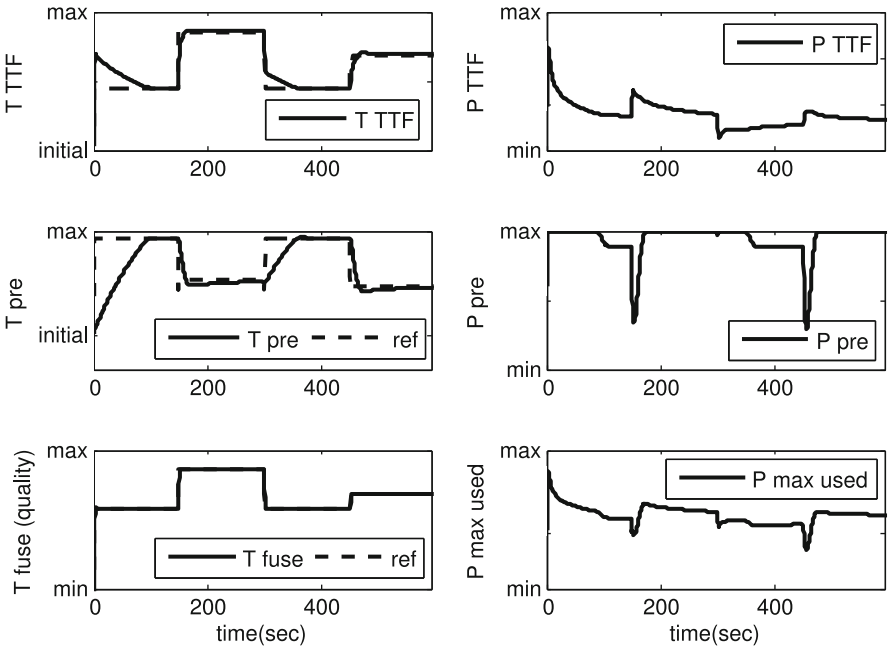

Fig. 4.25 MPC-decomposed: Temperatures in presence of mass variation

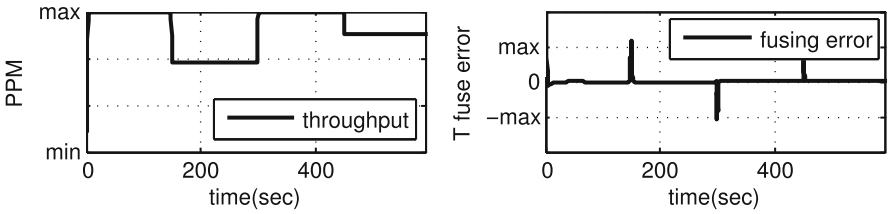

Fig. 4.26 MPC-decomposed: Productivity and fuse error for mass variation

4.4.3.2 Decomposed Model Predictive Control

The results of the decomposition of the plant model are presented next. The reference generator calculates each sample time k the optimal steady-state input $(v, d, P_{\text{pre}}, P_{\text{TTF}})$, based on the non-linear static model. The decoupled inputs, v and d, are sent directly to the system in feedforward. The MPC controller manages to track the setpoints accurately, denoting the robustness of the controller. The system remains stable under all conditions and delivers high performance. The computation time in this case is not a problem (maximum 0.15 seconds per sample) and the linear MPC is robust enough to compensate for modelling uncertainties.

Figures 4.25–4.27 show the results for the variation in the mass of the paper from Fig. 4.17. In this case, the references are calculated by the reference generator.

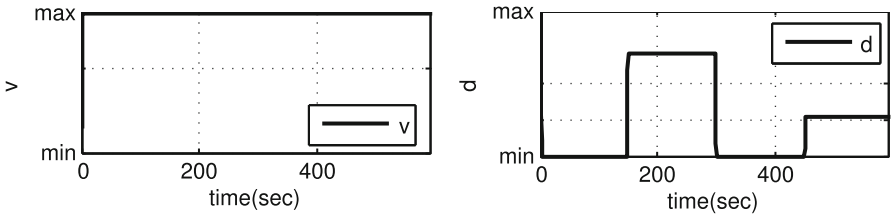

Fig. 4.27 MPC-decomposed: Belt speed and distance between sheets with mass variations

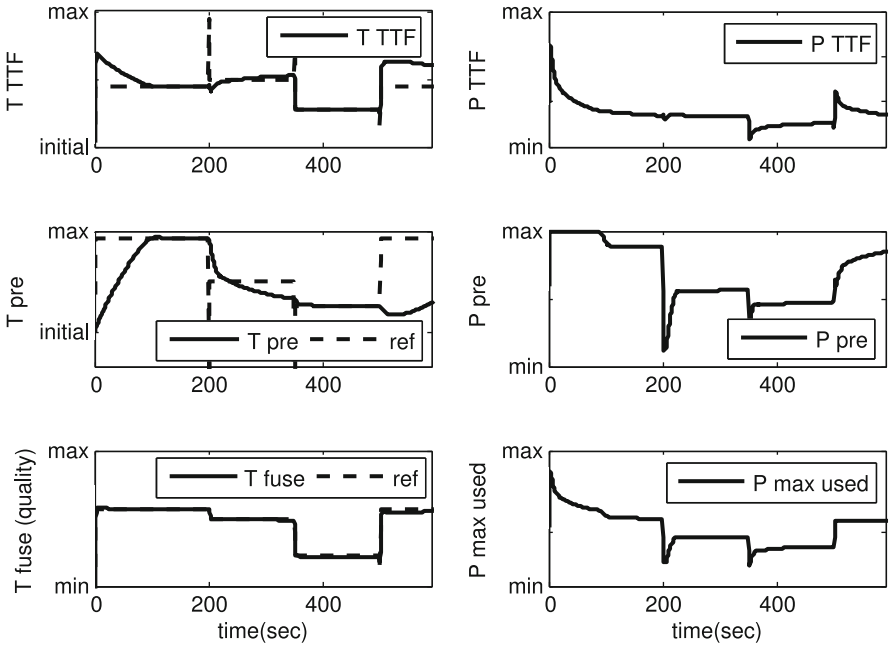

Fig. 4.28 MPC-decomposed: Temperatures in presence of $P_{\max}$ variation

The throughput has been adjusted to fulfil all requirements in a steady-state situation. The error in fuse quality is within specifications most of the time except for some transient situations. As we can see, for the case when the paper characteristics do not change so often, the system can be considered linear and then the decomposed controller will give a good performance.

Figures 4.28–4.30 show the results for the variation in the maximum available power from Fig. 4.21. The throughput will be adjusted to fulfil all requirements in steady state. The error in fuse quality is within specs most of the time.

To conclude this section, the implementation of both MPC strategies shows an improved performance of the printing system. Since the centralised MPC scheme solves a centralised non-linear dynamic optimisation problem, it requires

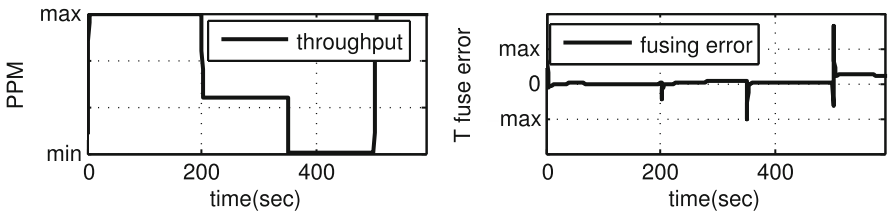

Fig. 4.29 MPC-decomposed: Productivity and fuse error in presence of $P_{\max}$ variation

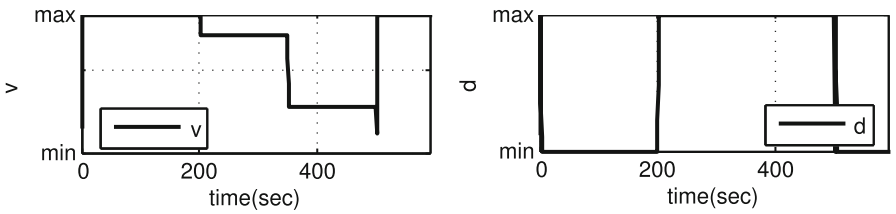

Fig. 4.30 MPC-decomposed: Belt speed and distance between sheets with $P_{\max}$ variation

a large computation time. The computation time can be reduced by decomposing the non-linear dynamic optimisation into a non-linear static optimisation and linear dynamic optimisation. That makes the decomposed MPC scheme more attractive for real-time implementation for the printing system. However, in case of large transitions of media type, the optimality of the solution is sacrificed in the transient performance due to the static optimisation.

4.5 Conclusions

The control design considerations have been discussed for selecting appropriate design methods for adaptive embedded systems, especially for professional toner printers. It has been shown that this class of systems is characterised by a deterministic physics-based model with changing and partly unknown parameters, many constraints, and partly-known disturbances. It has been argued that this class of systems benefits from deterministic control approaches as stochastic approaches cannot sufficiently exploit the existing knowledge. When comparing the deterministic control design methods, as shown in Fig. 4.31, adaptive methods are preferred as they can adapt their control behaviour to the changing operating conditions of a printer. Adaptation allows accurate control. The only requirement is that the adaptation is fast enough to follow the changing operating conditions. To speed up convergence, two new adaptation mechanisms for model reference adaptive control (MRAC) have been described and demonstrated. One mechanism is based on a non-linear gain and the second one is based on multiple gains depending on the operating condition. Especially, when the changing operating condition is

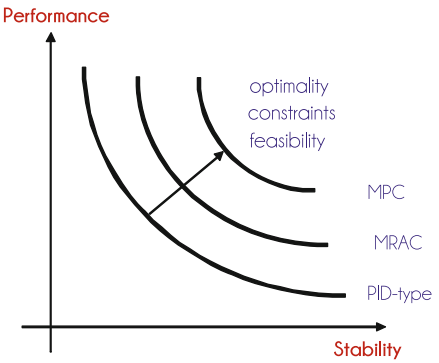

Fig. 4.31 Comparison of different control strategies

known (which is partly true for industrial printers), the multiple gain solution has a clear advantage, as it can adapt faster to changes in the print queue.

Another approach is based on adaptive model predictive control (MPC). This control approach allows the inclusion of all relevant knowledge to maximise the throughput of the printer while still satisfying the strict constraints on print quality and power consumption. Moreover, MPC allows the inclusion of knowledge of the known future disturbance owing to the print jobs in the print queue. A number of examples show the benefits of the new proposed approaches. It can be expected that applying MPC for the industrial electro-photography printer will improve performance considerably compared to the present control approach, based on PI-control and many heuristics. Besides an improved performance, so a higher throughput while satisfying the constraints, the design cycle of the controller will become shorter and leads to more structured design methodology. This means that in one consistent and transparent problem formulation all aspects concerning the operation of a printer can be taken into account. A solution of this large optimisation problem is feasible in real-time and yields the optimal compromise between all conflicting requirements.

Acknowledgements This work has been carried out as part of the Octopus project with Océ-Technologies B.V. under the responsibility of the Embedded Systems Institute. This project is partially supported by the Netherlands Ministry of Economic Affairs, Agriculture, and Innovation under the BSIK program.

References

1. Astrom, K.J., Wittenmark, B.: Adaptive Control. Addison-Wesley, Boston (1995)
2. Boyd, S., Vandenberghe, L.: Convex Optimization. Cambridge University Press, Cambridge (2004)
3. Butler, H.: Model Reference Adaptive Control: From Theory to Practice. Prentice Hall International, Upper Saddle River (1992)
4. Cao, S., Rees, N., Feng, G.: Analysis and design of fuzzy control systems using dynamic fuzzy global models. Fuzzy Sets Syst. **75**, 47–62 (1995)

5. Cochior, C., van den Bosch, P.P.J., Waarsing, R., Verriet, J.: Control strategy for systems with input-induced nonlinearities: A printing system case study. In: Proceedings of the 2012 American Control Conference (ACC 2012), Montreal, pp. 1949–1954 (2012)
6. Dessauer, J.H., Clark, H.E.: Xerography and Related Processes. The Focal Press, New York (1965)
7. Ezzeldin, M.: Performance improvement of professional printing systems: From theory to practice. Ph.D. thesis, Eindhoven University of Technology, Eindhoven (2012)
8. Ezzeldin, M., van den Bosch, P.P.J., Waarsing, R.: Improved convergence of MRAC design for printing system. In: Proceedings of the 2009 American Control Conference (ACC 2009), St. Louis, pp. 3232–3237 (2009)
9. Ezzeldin, M., Weiland, S., van den Bosch, P.P.J.: Robust $\mathscr{L}_2$ control for a class of nonlinear systems: A parameter varying Lyapunov function approach. In: Proceedings of the 19th Mediterranean Conference on Control and Automation (MED 2011), Corfu, pp. 213–218 (2011)
10. Ezzeldin, M., Weiland, S., van den Bosch, P.P.J.: Improving the performance of a printing system using model reference adaptive control: An LMI approach. In: Proceedings of the 2012 American Control Conference (ACC 2012), Montreal, pp. 1943–1948 (2012)
11. Ezzeldin, M., Weiland, S., van den Bosch, P.P.J.: Observer-based robust $\mathscr{L}_2$ control for a professional printing system. In: Proceedings of the 2012 American Control Conference (ACC 2012), Montreal, pp. 1955–1960 (2012)
12. Ferramosca, A., Limon, D., Alvarado, I., Almo, T., Camacho, E.F.: MPC for tracking of constrained nonlinear systems. In: Proceedings of the Joint 48th IEEE Conference on Decision and Control (CDC 2009) and the 28th Chinese Control Conference (CCC 2009), Shanghai, pp. 7978–7983 (2009)
13. Fridkin, V.M.: The Physics of The Electrophotographic Process. The Focal Press, New York (1972)
14. Groot, P., Birlutiu, A., Heskes, T.: Learning from multiple annotators with Gaussian processes. In: Honkela, T., Duch, W., Girolami, M., Kaski, S. (eds.) Artificial Neural Networks and Machine Learning ICANN 2011. Lecture Notes in Computer Science, vol. 6792, pp. 159–164. Springer, Heidelberg (2011)
15. Groot, P., Lucas, P., van den Bosch, P.: Multiple-step time series forecasting with sparse Gaussian processes. In: Proceedings of the 23rd Benelux Conference on Artificial Intelligence (BNAIC 2011), Ghent, pp. 105–112 (2011)
16. Heemels, M., Muller, G.: Boderc: Model-Based Design of High-Tech Systems. Embedded Systems Institute, Eindhoven (2007)
17. Krijnen, B.: Heat flow modelling in copiers. Master's thesis, University of Twente, Enschede (2007)
18. Lazar, M., Gielen, R.: On parameterised Lyapunov and control Lyapunov functions for discrete-time systems. In: Proceedings of the 49th IEEE Conference on Decision and Control (CDC 2010), Atlanta, pp. 3264–3270 (2010)
19. Li, D., Xi, Y.: The feedback robust MPC for LPV systems with bounded rates of parameter changes. IEEE Trans. Autom. Control **55**, 503–507 (2010)
20. Lienhard IV, J.H., Lienhard V, J.H.: A Heat Transfer Textbook. The Phlogiston Press, Cambridge (2004)
21. Maciejowski, J.M.: Predictive Control with Constraints. Pearson Education, Upper Saddle River (2002)
22. Magni, L., Scattolini, R.: On the solution of the tracking problem for non-linear systems with MPC. Int. J. Syst. Sci. **36**, 477–484 (2005)
23. MATLAB: http://www.mathworks.com/products/matlab/. Accessed Aug 2012
24. Mayne, D.Q., Rawlings, J.B., Rao, C.V., Scokaert, P.O.M.: Constrained model predictive control: Stability and optimality. Automatica **36**, 789–814 (2000)
25. Nounou, H.N., Passino, K.M.: Stable auto-tuning of the adaptation gain for continuous-time nonlinear systems. In: Proceedings of the 40th IEEE Conference on Decision and Control (CDC 2001), Orlando, pp. 2037–2042 (2001)

26. Takagi, T., Sugeno, M.: Fuzzy identification of systems and its applications to modelling and control. IEEE Trans. Syst. Man Cybern. **15**, 116–132 (1985)
27. Tanaka, K., Sugeno, M.: Stability analysis and design of fuzzy control systems. Fuzzy Sets Syst. **45**, 135–136 (1992)
28. Thathachar, M.A.L., Gajendran, F.: Convergence problems in a class of model reference adaptive control systems. In: Proceedings of the 1977 Conference on Decision and Control (CDC 1977), Bangalore, pp. 1036–1041 (1977)
29. Wang, L.: A Course in Fuzzy Systems and Control. Prentice Hall, London (1997)
30. Williams, M.E.: The Physics and Technology of Xerographic Processes. Wiley, New York (1984)
31. Yu, S., Bohm, C., Chen, H., Allgower, F.: Stabilizing model predictive control for LPV systems subject to constraints with parameter-dependent control law. In: Proceedings of the 2009 American Control Conference (ACC 2009), St. Louis, pp. 3118–3123 (2009)